Arch. Metall. Mater. **70** (2025), 2, 609-616

DOI: https://doi.org/10.24425/amm.2025.153462

G. YUAN[1*], C. YAN[1], H. WU[2], X. XIAO[3], S. ZHAO[1], Z. YU[1]

STUDY ON MICROSTRUCTURE AND HOT DEFORMATION BEHAVIOR OF HIGH CHROMIUM CAST IRON/LOW CARBON STEEL LAMINATE

A hot compression process was developed to study the hot deformation behavior and microstructure of a high chromium cast iron/low carbon steel laminate on a Gleeble 3800 thermal simulation test machine at a temperature of 950-1200°C. The deformation characteristics and the microstructure evolution of the specimens were investigated. Experimental results showed that the monolithic high chromium cast iron specimen cracked during hot compression, but the formability of brittle cast iron in the core of the sandwich structure was improved. Besides, the two metals showed better coordination deformation performance after hot compression treatment at 1150°C. The simultaneous deformation of high chromium cast iron and the ductile carbon steel changed the deformation mode of the cast iron and reduced the normal stress that the cast iron bore. The coarse carbides in cast iron fractured and dissolved into the matrix after hot compression. The interface between the two metals was well bonded without any interfacial cracks and voids produced, forming a corrugated shape.

Keywords: Hot compression; High chromium cast iron; Microstructure; Bonding interface

1. Introduction

High chromium cast iron (HCCI) is an excellent wear-resisting material, which has been extensively applied in mining, metallurgy, electric power and other engineering fields [1,2]. The exceptional wear resistance of HCCI is mainly attributed to its high volume fraction of M_7C_3 carbides [3,4]. However, those hard and continuous carbides greatly reduce the deformation capacity and impact resistance of HCCI. Cracks and fractures would occur on the surface of HCCI even if it was hot worked at high deformation temperatures [5]. Usually, the cast iron cannot be deformed in metal forming processes. The inherent brittleness and poor thermal deformation ability of cast iron not only cumber its widespread application in engineering, but also make it difficult to improve the microstructure through the thermoplastic deformation process. In order to improve the comprehensive mechanical properties of HCCI, heat treatment [6,7], spray casting [8] and micro-alloying [9-11] are often adopted to refine the carbide in HCCI.

Due to the poor plastic deformation ability of HCCI, few researchers have refined the microstructure of HCCI using thermal deformation processes such as rolling or forging. Wang et al. [12] performed thermal compression deformation of HCCI (Cr 14.4%) at 450°C with a strain of 20%. The results suggested that the hard M_7C_3 carbide underwent certain plastic deformation during the deformation process, and dislocations and twins were observed in the M_7C_3 carbide. Pei et al. [13] claimed that the brittle HCCI had high potential for thermal deformation. During the process of hot compression deformation, the HCCI could release stress through the fracture of coarse M_7C_3 carbides, and the softened fine carbide and austenite matrix showed a good "self-healing effect" on cracks. This "self-healing effect" could make HCCI obtain good deformation performance to some extent. Jiang and Gao et al. [14,15] examined the influence of hot pressing deformation at different temperatures on the morphology and distribution of primary carbides in HCCI through hot compression simulation experiment. After hot pressing deformation, the long axis of M_7C_3 carbides in HCCI ended to be align with the deformation direction, and some primary carbides rotated by 90°. Xie et al. [16] produced a LCS/HCCI/LCS composite plate through sand casting, which was then subjected to multi-pass hot rolling deformation. According to their research results, the microstructure of cast iron was significantly refined after hot rolling deformation, and partially broken M_7C_3 carbide

[1] SCHOOL OF MECHANICAL ENGINEERING, ANYANG INSTITUTE OF TECHNOLOGY, ANYANG 455000, CHINA
[2] HENAN ZHENGSHANG CONSTRUCTION ENGINEERING CO., LTD., ANYANG 455000, CHINA
[3] HENAN ANCAI HI-TECH CO., LTD., ANYANG 455000, CHINA

* Corresponding author: aygxyygf@163.cn

was dissolved in the austenitic matrix. Similarly, Liu et al. [17] fabricated a sandwich-structured composite containing a brittle HCCI core and LCS claddings through centrifugal casting and hot-rolling methods. The results indicated that good metallurgical bonding was achieved between the two metals after centrifugal composite casting. The initial casting binding interface had a certain constraint effect on the HCCI in the core layer, and the stress release effect of the softer carbon steel layer in the sandwich structure reduced the crack sensitivity of the HCCI. Therefore, in the subsequent hot rolling deformation process, the HCCI in the core showed good plastic deformation performance without producing macroscopic cracks.

In the present research, a laminate composite containing the HCCI core and LCS claddings was fabricated through the hot compression process on a Gleeble 3800 thermal simulation test machine at a temperature of 950-1200°C. The hot deformation behavior of HCCI was discussed. The microstructure of the composite was investigated using an optical microscope (OM) and scanning electron microscope (SEM).

2. Experimental procedures

The as-cast HCCI and commercial hot-rolled carbon steel were chosen as research objects, and their chemical compositions were given in TABLE 1.

TABLE 1

Chemical compositions (wt.%) of HCCI and LCS

Material	C	Si	Cr	Mn	P	S	Mo	Ni	Fe
HCCI	2.8	1.1	28	1.0	0.02	0.02	0.5	0.4	balance
LCS	0.12	0.2	0.1	0.5	0.01	0.002	—	—	balance

Gleeble 3800 thermal simulator was used for the hot compression and hot deformation experiments. The HCCI and carbon steel specimens of 6 mm diameter and 5 mm thickness were prepared. The specimen surface was polished with 1μm diamond finish and then cleaned by alcohol. Afterwards, the two metals were stacked to form the LCS/HCCI/LCS structure. The assembled three-layer-stacked cylindrical specimens were placed in a steel sleeve with an inner diameter of 6mm to ensure the coaxiality of the three layers. The assembling diagram of the two metals and the thermal deformation process are shown in Fig. 1. During the experiment, 30% of thickness reduction of the assembly was carried out in each test. The temperature of the test was raised from 950°C to 1200°C, an increase of 50°C each time, and the strain rate was $0.01s^{-1}$. The thermal compression deformation experiment was carried out in a low vacuum environment, and the specimens were air-cooled to room temperature after the test. The monolithic HCCI specimen of 10 mm diameter and 12 mm length was subjected to the hot compression test as a comparison.

To examine the deformation property and the bonding quality of the two metals, the specimens after hot deformation were wire wire-cut across the Y-Z plane (Fig. 1(b)), and then polished with 1μm diamond finish and cleaned by ethanol. The metallographic specimens were polished and etched by a 4% nitric acid alcohol solution. The microstructure of the test specimens was analyzed using the OM and SEM.

3. Results and discussion

3.1. Hot deformation behavior

As a brittle material with high crack sensitivity, monolithic HCCI can hardly achieve good thermoplastic deformation performance. The monolithic HCCI specimen crack and was crushed when treated under 30% of thickness reduction at 1000°C, as shown in Fig. 2. The upper and lower ends of the specimen did not deform, but the middle of the cylinder collapsed. Apart from reflecting the deformation characteristics of materials, the true stress-strain curve is also a representation of the material structure and property changes. Fig. 3(a) shows the true stress-strain curves of the monolithic HCCI subject to 30% thickness reduction treatment at different temperature. As can be seen, the true stress increased rapidly during the deformation process.

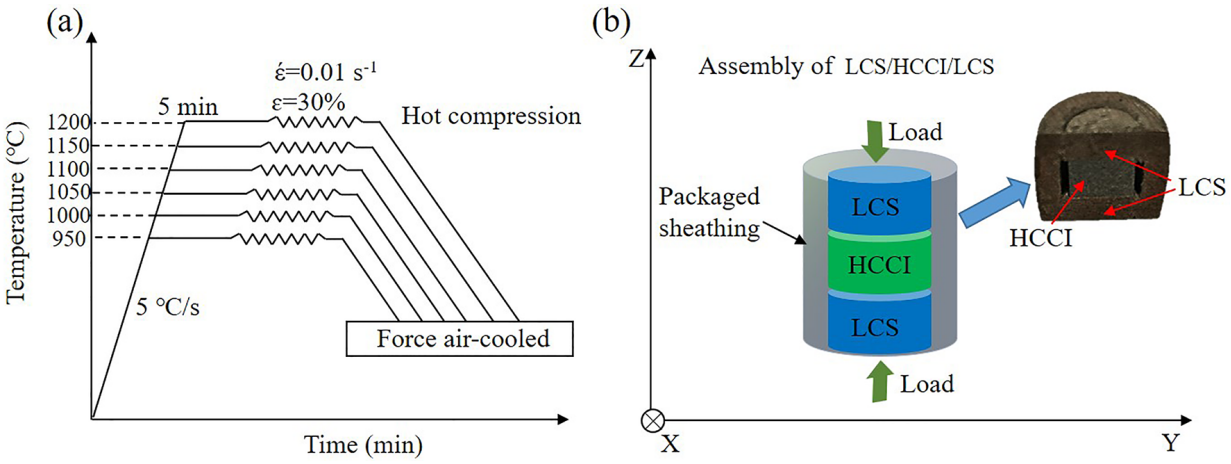

Fig. 1. (a) Schematic diagram of laminate hot compression deformation process and (b) schematic diagram of sample assembly

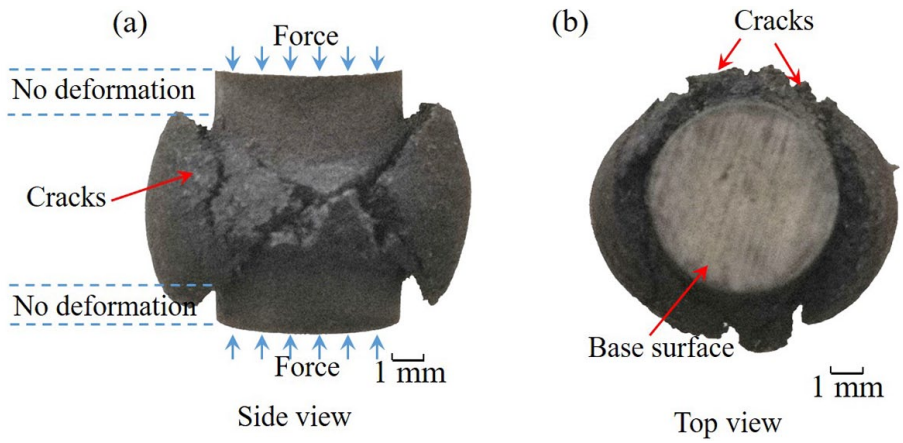

Fig. 2. The macroscopic morphology of the monolithic HCCI under 30% of thickness reduction at 1000℃: (a) side view and (b) top view

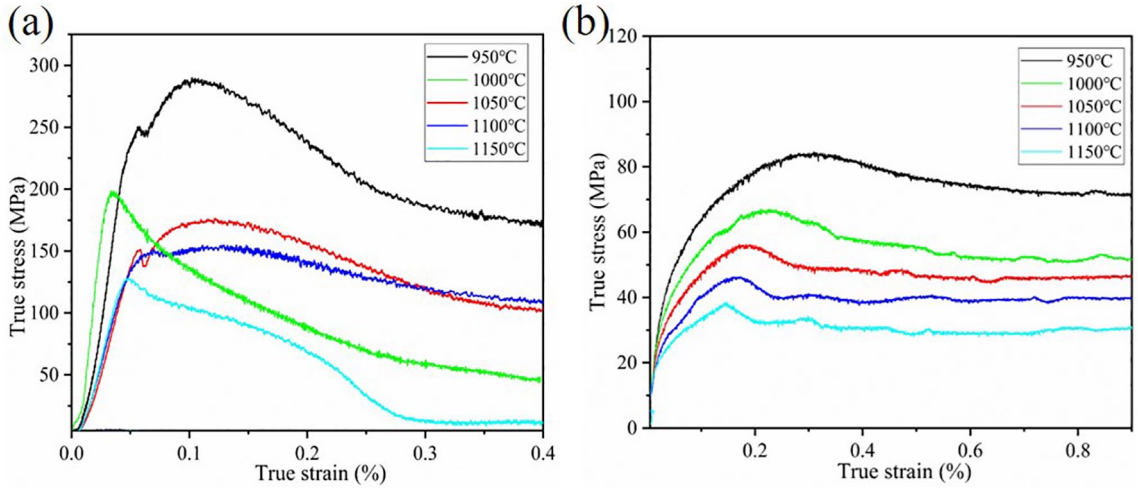

Fig. 3. The true stress-strain curve of the two metals with the strain rate of 0.01 s^{-1} at different temperature: (a) HCCI and (b) LCS

However, the stress subsequently decreased with the increase of strain. The fluctuation of the curve was mainly related to crack formation and propagation in the material. Fig. 3(b) shows the true stress-stain curves of LCS at different temperature. It can be seen that the flow stress of LCS decreases with the increase of temperature. At the initial stage of deformation, the flow stress increases rapidly with the increase of strain, which is caused by dislocation and work hardening. After that, the flow stress increases slowly to the peak and remains stable.

In order to analyze the effect of hot pressing deformation on the microstructure of HCCI, the specimen was processed by wire cutting along the loading direction (Y-Z). Fig. 4(a) shows the OM image of the monolithic HCCI before hot deformation. It can be seen from the figure that a large number of rod-shaped primary and eutectic carbides were distributed in the matrix of HCCI. The cross-section of the primary carbide was irregular hexagon or polygon shaped. The high carbide volume fraction in HCCI made it easy to crack along the brittle carbide during

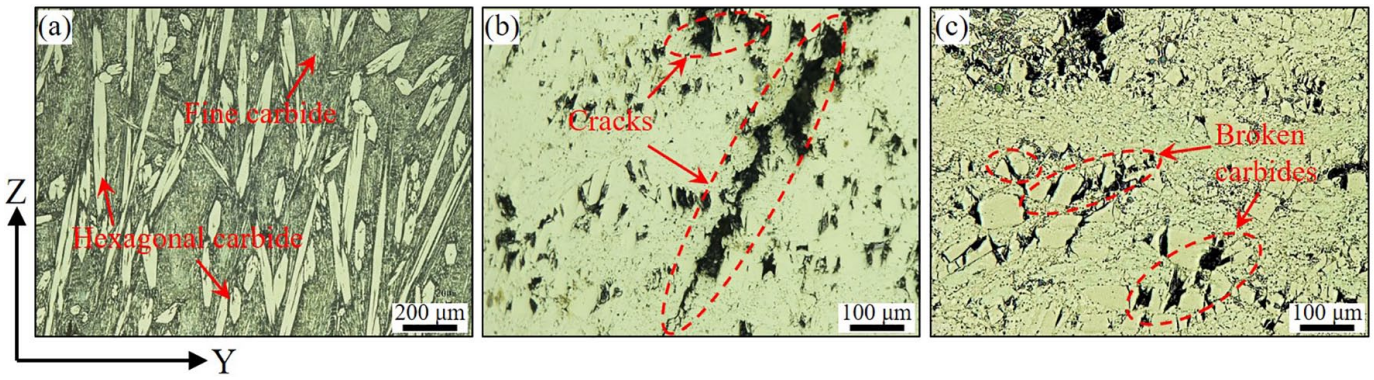

Fig. 4. Microstructure of the monolithic HCCI: (a) before hot deformation, (b) and (c) after hot compression

deformation [18]. Figs. 4(b,c) are the OM images of the monolithic HCCI after hot deformation. According to the figure, there were many cracks in HCCI after deformation. A majority of primary carbides fractured into two or more small pieces, and micro-cavities or cracks without matrix filling were formed between the fractured carbides (Fig. 4(c)).

After hot compression, the laminate specimens were wire-cut along the direction of the applied load (Y-Z). In order to show the deformation of the two metals more directly, the section surface of the sample was ground, polished and etched by a 4% nitric acid alcohol solution. Fig. 5 illustrates the macroscopic morphology of the laminate specimens after hot compression treatment at different temperatures. Because the deformation resistance of the two metals varied greatly at different temperatures (Fig. 3), evident difference in the thickness was found between the two metal layers after hot compression deformation. At the temperatures of 950°C, 1000°C and 1050°C, the deformation mainly occurred in the LCS layers, while the middle HCCI layer nearly underwent no deformation. This phenomenon indicated that when the thermal compression temperature was below 1050°C, the deformation resistance of the middle HCCI layer was markedly greater than that of the upper and lower LCS layers, and it was difficult for the two metals to achieve good coordination deformation performance. A clear gap was formed between the outer carbon steel cladding and the HCCI in the core, and the LCS layer had a tendency to squeeze into the gap (Figs. 5(a-c)). It was mainly because the upper and lower LCS layers deformed greatly and expanded in the radial direction during hot compression.

The compression deformation still predominantly occurred in the LCS layers at 1100°C, but drum deformation was observed in the circumferential area of the HCCI core (Fig. 5(d)). In addition, the gap between the HCCI core and carbon steel claddings narrowed with the increase of temperature. It indicated that the difference in the deformation resistance between LCS and HCCI decreased with the elevating temperature. Both HCCI and LCS underwent obvious plastic deformation at 1150°C, and the gap between the HCCI core and the outer carbon steel claddings disappeared. Moreover, after hot compression deformation at 1150°C, the cross section of the HCCI layer in the core was intact without any macroscopic cracks and other defects in it (Fig. 5(e)). However, when the thermal deformation temperature rose to 1200°C, some large cavity defects were generated in the core HCCI layer, a result of local melting of HCCI at this temperature.

In order to further analyze the difference in the thickness and percent deformation between the two layers after hot pressing deformation at different temperatures, the thickness of two layers of the specimen after hot compression was measured by using a measuring microscope. Fig. 6(a) describes the relationship between the layer thickness and temperature of the two metals after hot compression deformation. When the thermal deformation temperature was between 950°C-1050°C, the deformation mainly occurred in the soft LCS layer. With the increase of the deformation temperature, the difference in the thickness and percent deformation between the two metal layers gradually decreased. Especially at the temperature of 1150°C, the two metals showed better coordination deformation performance (Fig. 6(b)).

Compression deformation is similar to an upsetting process, in which surface cracking is often caused by uneven deformation

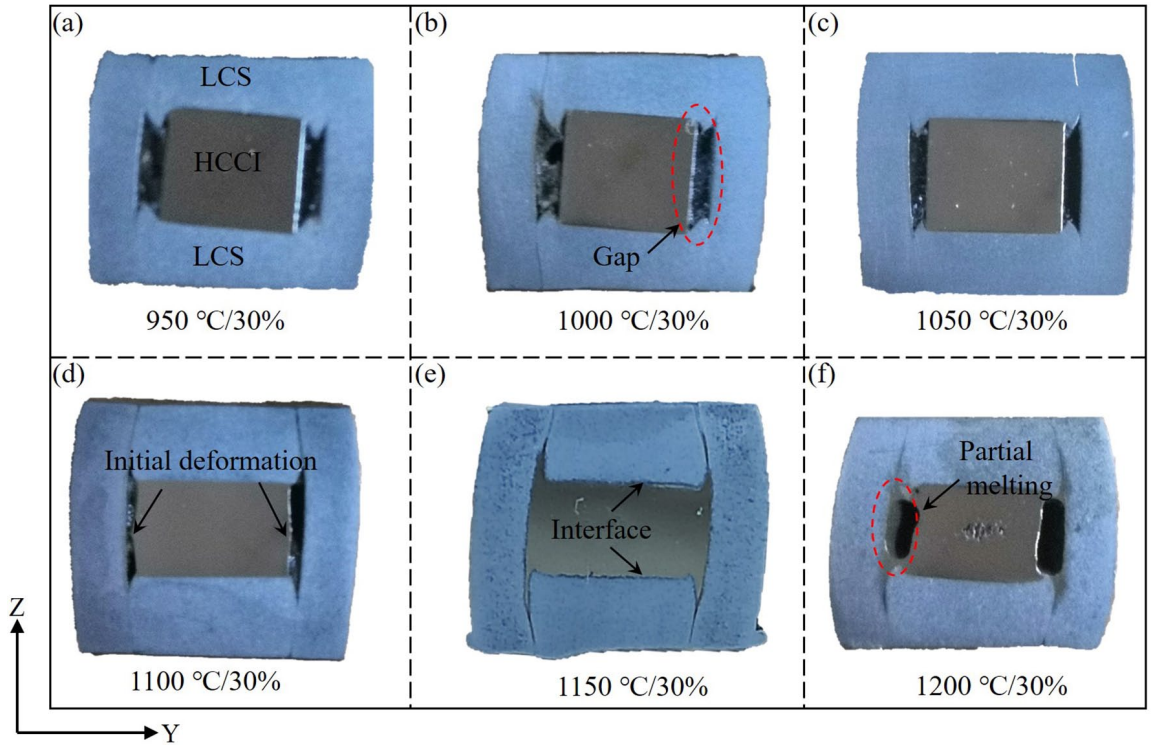

Fig. 5. Macrographs of the laminate composite after thermal compression at different temperatures: (a) 950°C, (b) 1000°C, (c) 1050°C, (d) 1100°C, (e) 1150°C, (f) 1200°C

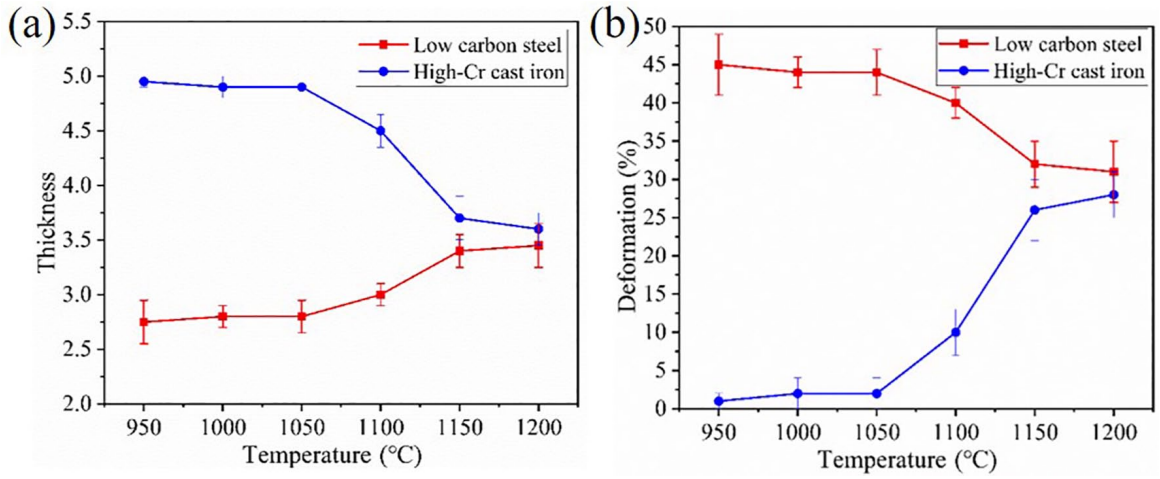

Fig. 6. (a) Relationship between the layer thickness and temperature and (b) relationship between the deformation and temperature

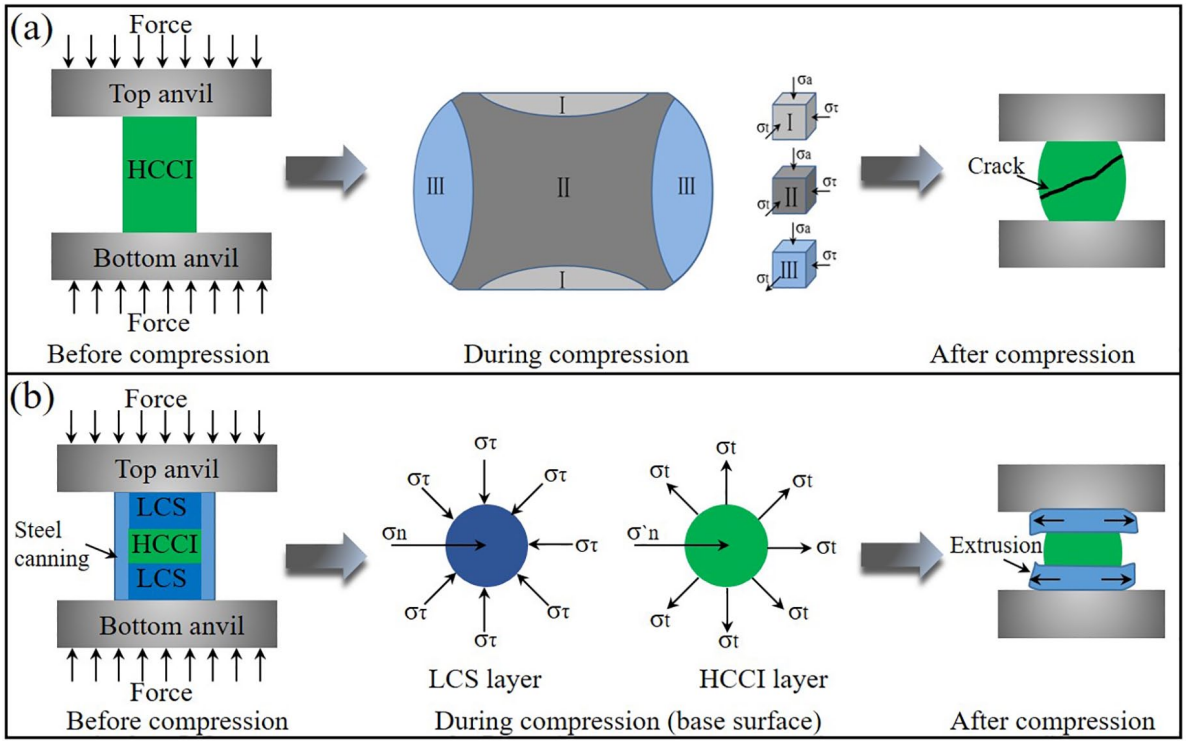

Fig. 7. Schematic diagram of hot compression: (a) the monolithic HCCI and (b) the laminate composite

of structures within the material. Fig. 7 shows the schematic diagram of hot pressing the monolithic HCCI and the laminate composite. According to the mechanics of plastic forming, the longitudinal section of the cylindrical specimen after compression deformation can be approximately divided into three different deformation zones by the macroscopic deformation degree (Fig. 7(a)) [19,20]. During the deformation, the friction between the anvils and the specimen tended to prevent the radial expansion of the specimen, and a dead-metal zone was formed at both the top and the bottom. Thus, the specimen bore various stresses during deformation. The core of the specimen was subjected to triaxial compressive stress, while the barreling region of the specimen suffered normal and tensile stresses in radial directions. The uneven distribution of stress or strain during compression deformation often leads to the non-uniformity of microstructure distribution in the deformation process. Besides, lateral cracks would form as the flow stress or plastic strain in the barreling region exceeds the critical value.

Improving the material deformation uniformity can reduce the number of defects formed to a certain extent. Hot deformation altered the deformation mode of the HCCI core (Fig. 7(b)). Since the LCS layers have excellent deformation ability at high temperatures, the friction at the interface between the LCS layer and the HCCI layer tended to enforce simultaneous deformation of the HCCI core and the steel in contact with it. The tensile stress acted on the base surface of HCCI would facilitate its extension, thus inhibiting the formation of the dead-metal zones at the top and the bottom, and reducing the normal stress in HCCI [21-23].

3.2. Microstructure evolution

Fig. 8 shows the OM images of the hot compression bonding interface between HCCI and LCS. The upper side is LCS and the lower side is HCCI. It can be seen that the microstructure differed greatly at different temperatures. At a low thermal deformation temperature (950-1050°C), the microstructure of the HCCI core layer was similar to that of as-cast specimen. In the deformation temperature range, the HCCI was composed of the soft austenitic matrix and a high volume fraction of hard M_7C_3 carbides. During the process of hot deformation, the hard M_7C_3 carbide played a supporting role and increased the HCCI resistance against deformation. At the bonding interface, the positive pressure exerted by the LCS layer made the hard Cr-carbide protrude from the matrix surface, resulting in a large number of primary carbides being embedded in the LCS layer. Thus, the bonding interface between the two metals was similar to rolling peaks (Fig. 8(b)).

Compared with that in the samples subjected to hot deformation at 950°C and 1050°C, the size of carbides in HCCI of the specimen treated at the deformation temperature of 1150°C was relatively small. Besides, the interface between the two metals was flatter at 1150°C. Furthermore, only a small quantity of carbides were embedded in the LCS layer, and some carbides near the interface were obviously bended at 1150°C (Fig. 8(d)). The above phenomena demonstrated that the difference in the hardness between the carbide and matrix in HCCI decreased with the increase of temperature, and the hard carbide phase and the matrix had slight plastic deformation. Wang et al. [12] found that M_7C_3 carbides in HCCI would undergo plastic deformation before fracture rather than directly fracture.

Fig. 9 presents the SEM images of the hot compression bonding interface between HCCI and LCS. The left side is LCS and the right side is HCCI. The two metals were well bonded, and no defects such as delamination and interfacial cracks were observed. With the increase of the thermal deformation temperature, the number of carbides embedded in the LCS layer gradually decreased, and the interface between the two metals undulated slight (Fig. 9(d)). In addition, partially dissolved and separated M_7C_3 carbides (marked with black circles in Fig. 9(d)) were observed in the HCCI layer. Gavriljuk et al. [24] studied the decomposition of cementite in pearlitic steel during plastic deformation and demonstrated the dissolution of the hard phase during high temperature deformation.

The morphological changes of carbides in HCCI after hot compression deformation are attributed not only to the carbide fracture and breakage during the compression deformation process, but also to the carbide dissolution and separation in hot deformation [17]. As shown in Fig. 8 and Fig. 9, after deformation at high temperatures, the carbide sharp angle was rounded and there were many small and irregular massive carbides distributed in the matrix. These phenomena indicated that the carbides dissolved

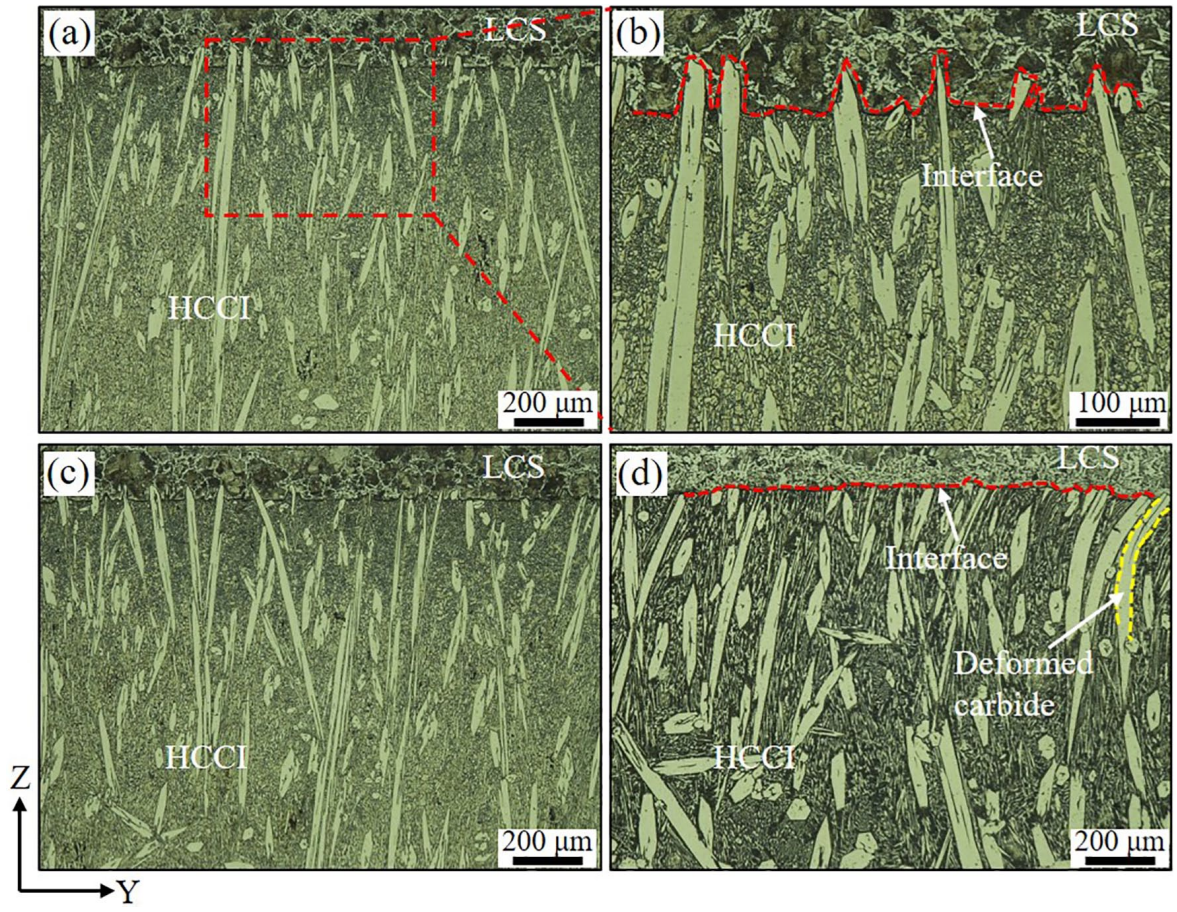

Fig. 8. Optical microstructure of hot compression bonding interface between HCCI and LCS: (a) and (b) 950°C, (c) 1050°C, (d) 1150°C

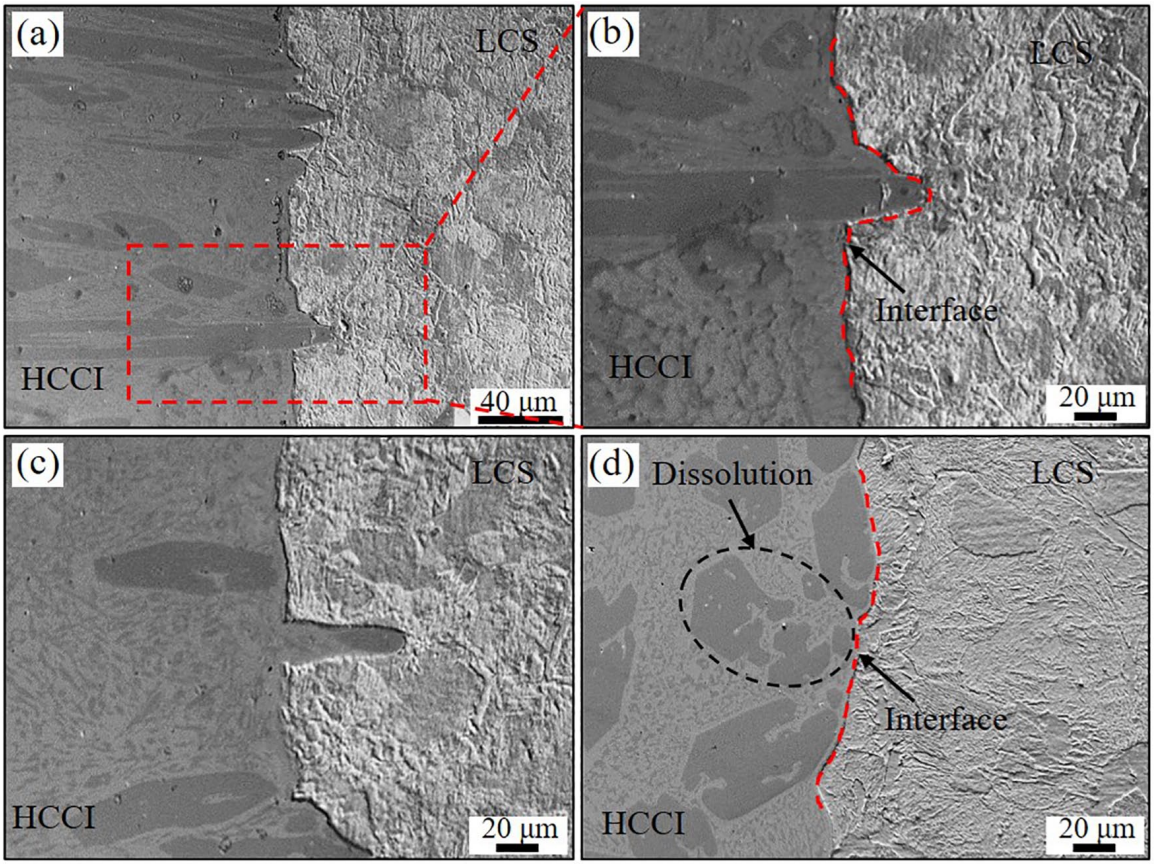

Fig. 9. SEM microstructure of hot compression bonding interface between HCCI and LCS: (a) and (b) 950℃, (c) 1050℃, (d) 1150℃

in the process of high temperature deformation. In Fig. 8(d), the holes in the central matrix of the carbide gradually expanded, and the hexagonal carbide dissolved and separated into two or more irregular-shaped masses. During the deformation process, the dissolved and separated carbide masses further separated, flew and rotated with the flow of the matrix. The microstructure refinement of HCCI during hot compression deformation was the result of carbide dissolution, separation and fracture.

4. Conclusions

The hot deformation behavior and microstructure of the monolithic HCCI and HCICI/LCS bimetal was analyzed. The following conclusions can be draw from this work.

(1) The monolithic HCCI specimen cracked and was crushed by hot compression treatment. For the HCCI/LCS laminate, the deformation mainly occurred in the LCS layers when the bonding temperature was at or below 1050 ℃. With the increase of the thermal deformation temperature, the difference in the thickness between the two metal layers decreased gradually, and the two metals showed better coordination deformation performance at 1150℃.

(2) Hot deformation improved the formability of the HCCI core layer. The simultaneous deformation of HCCI and ductile LCS changed the deformation mode of HCCI and relieved the normal stress in HCCI.

(3) The interface between the two metals was well bonded without any interfacial cracks and voids formed, presenting a corrugated or undulating shape. The carbides in HCCI fractured and dissolved during the hot deformation process.

Acknowledgments

This work was funded by the Henan Science and Technology Plan Project (No. 232102230060, 232300420325) and the Doctoral Research Start-Up Fund of the Anyang Institute of Technology (No. BSJ2023003).

REFERENCES

[1] S.D. Carpenter, D. Carpenter, J.T.H. Pearce, XRD and electron microscope study of an as-cast 26.6% chromium white iron microstructure. Mater. Chem. Phys. **85**, 32-40 (2004). DOI: https://doi.org/10.1016/j.matchemphys.2003.11.037

[2] R.J. Llewellyn, S.K. Yick, K.F. Dolman, Scouring erosion resistance of metallic materials used in slurry pump service. Wear **256**, 592-599 (2004). DOI: https://doi.org/10.1016/j.wear.2003.10.002

[3] I. Fernández, F.J. Belzunce, Wear and oxidation behaviour of high-chromium white cast irons. Mater. Charact. **59**, 669-674 (2008). DOI: https://doi.org/10.1016/j.matchar.2007.05.021

[4] A. Bedolla Jacuinde, W.M. Rainforth, The wear behaviour of high-chromium white cast irons as a function of silicon and Mischmetal content. Wear **250**, 449-461 (2001). DOI: https://doi.org/10.1016/S0043-1648(01)00633-0

[5] Z.Y. Jiang, X.J. Gao, S.L. Li, H.M. Zhang, D.F. Chen, J.Z. Xu, Interface Analysis and Hot Deformation Behavior of a Novel Laminated Composite with High-Cr Cast Iron and Low Carbon Steel Prepared By Hot Compression Bonding. J. Iron. Steel. Res. Int. **22**, 438-445 (2015). DOI: https://doi.org/10.1016/S1006-706X(15)30024-8

[6] V. Efremenko, K. Shimizu, Y. Chabak, Effect of Destabilizing Heat Treatment on Solid-State Phase Transformation in High-Chromium Cast Irons. Metall. Mater. Trans. A 44,5435-5446 (2013). DOI: https://doi.org/10.1007/s11661-013-1890-9

[7] H. Gasan, F. Erturk, Effects of a Destabilization Heat Treatment on the Microstructure and Abrasive Wear Behavior of High-Chromium White Cast Iron Investigated Using Different Characterization Techniques. Metall. Mater. Trans. A **44**, 4993-5005 (2013). DOI: https://doi.org/10.1007/s11661-013-1851-3

[8] T.R. Matsuo, C.S. Kiminami, W.J. Botta Fa, C. Bolfarini, Sliding wear of spray-formed high-chromium white cast iron alloys. Wear **259**, 445-452 (2005). DOI: https://doi.org/10.1016/j.wear.2005.01.021

[9] R.J. Chung, X. Tang, D.Y. Li, B. Hinckley, K. Dolman, Effects of titanium addition on microstructure and wear resistance of hypereutectic high chromium cast iron Fe–25wt.%Cr–4wt.%C. Wear **267**, 356-61(2009). DOI: https://doi.org/10.1016/j.wear.2008.12.061

[10] X.H. Zhi, J.D. Xing, H.G. Fu, Y.M. Gao, Effect of titanium on the as-cast microstructure of hypereutectic high chromium cast iron. Mater. Charact. **59**, 1221-1226 (2008). DOI: https://doi.org/10.1016/j.matchar.2007.10.010

[11] E. Waleed, R. Rashad, E. Sayed, E. Saied, Influence of Vanadium and Boron Additions on the Microstructure, Fracture Toughness, and Abrasion Resistance of Martensite-Carbide Composite Cast Steel. Adv. Mater. Sci. Eng. **2016**, 1-8 (2016). DOI: https://doi.org/10.1155/2016/1203756

[12] J.D. Wang, W. Guo, H. Sun, H. Li, H.Y. Gou, J.W. Zhang, Plastic deformation behaviors and hardening mechanism of M_7C_3 Carbide. Mat. Sci. Eng. A **662**, 88-94 (2016). DOI: https://doi.org/10.1016/j.msea.2016.03.062

[13] Y. Pei, R.B. Song, Y.C. Zhang, L. Huang, C.H. Cai, E. Wen, Z.Y. Zhao, P. Yu, S.Y. Quan, S.R. Su, C. Chen, The relationship between fracture mechanism and substructures of primary M_7C_3 under the hot compression process of self-healing hypereutectic high chromium cast iron. Mat. Sci. Eng. A **779**, 139150 (2020). DOI: https://doi.org/10.1016/j.msea.2020.139150

[14] J.Z. Xu, X.J. Gao, Z.Y. Jiang, D.B. Wei, A Comparison of Hot Deformation Behavior of High-Cr White Cast Iron and High-Cr White Cast Iron/Low Carbon Steel Laminate. Steel. Res. Int. **87**, 780-788 (2015). DOI: https://doi.org/10.1002/srin.201500234

[15] X.J. Gao, Z.Y. Jiang, D.B. Wei, S.H. Jiao, D.F. Chen, J.Z. Xu, X.M. Zhang, D.Y. Gong, Effects of temperature and strain rate on microstructure and mechanical properties of high chromium cast iron/low carbon steel bimetal prepared by hot diffusion-compression bonding. Mater. Design **63**, 650-657 (2014). DOI: https://doi.org/10.1016/j.matdes.2014.06.067

[16] G.L. Xie, J.T. Han, J. Liu, Z.Y. Jiang, Texture, microstructure and microhardness evolution of a hot-rolled high chromium cast iron. Mat. Sci. Eng. A **527**, 6251-6254 (2010). DOI: http://dx.doi.org/10.1016/j.msea.2010.06.036

[17] F. Liu, Y.H. Jiang, H. Xiao, J. Tan, Study on fragmentation and dissolution behavior of carbide in a hot-rolled hypereutectic high chromium cast iron. J. Alloy. Compd. **618**, 380-385 (2015). DOI: https://doi.org/10.1016/j.jallcom.2014.07.131

[18] C.K. Kim, S. Lee, J. Jung, Effects of heat treatment on wear resistance and fracture toughness of duo-cast materials composed of high-chromium white cast iron and low-chromium steel. Metall. Mater. Trans. A **37**, 633-643 (2006). DOI: https://doi.org/10.1007/s11661-006-0035-9

[19] D.R. Lesuer, C.K. Syn, O.D. Sherby, J. Wadsworth, J.J. Lewandowski, W.H. Hunt, Mechanical behaviour of laminated metal composites, Int. Mater. Rev. **41**, 169-197 (1996). DOI: https://doi.org/10.1179/imr.1996.41.5.169

[20] S.H. Yan, Fundamental of Material Forming Process: Hot Working of Metals. Tsinghua University Press, Beijing 2005.

[21] N. Masahashi, S. Watanabe, S. Hanada, K. Komatsu, G. Kimura, Fabrication of iron aluminum alloy/steel laminate by clad rolling. Mater. Trans. A **37**, 1665-1673 (2006). DOI: https://doi.org/10.1007/s11661-006-0108-9

[22] Y.H. Jing, L.P. Luo, Fundamental of Mechanical Manufacture (Volume One). Tsinghua University Press, Beijing 2004.

[23] H. Yan, T.R. Zhou, Principle of Plastic Forming, Tsinghua University Press, Beijing 2008.

[24] V.G. Gavriljuk, Decomposition of cementite in pearlitic steel due to plastic deformation. Mater. Sci. Eng. A **345**, 81-89 (2003). DOI: https://doi.org/10.1016/S0921-5093(02)00358-1